REFERENCES AND NOTES

1. D. W. Choi, *Neuron* **1**, 623 (1988).
2. B. I. Kanner and S. Schuldiner, *CRC Crit. Rev. Biochem.* **22**, 1 (1987).
3. M. Szatkowski and D. Attwell, *Trends Neurosci.* **17**, 359 (1994); A. M. Palmer, A. W. Procter, G. C. Stratmann, D. M. Bowen, *Neurosci. Lett.* **66**, 199 (1986); J. D. Rothstein, M. V. Kammen, A. I. Levey, L. J. Martin, R. W. Kuncl, *Ann. Neurol.* **38**, 73 (1995); C. Portera-Cailliau, J. C. Hedreen, D. L. Price, V. E. Koliatsos, *J. Neurosci.* **15**, 3775 (1995).
4. T. Storck, S. Schulte, K. Hofmann, W. Stoffel, *Proc. Natl. Acad. Sci. U.S.A.* **89**, 10,955 (1992); G. Pines *et al.*, *Nature* **360**, 464 (1992); Y. Kanai and M. A. Hediger, *ibid.*, p. 467; K. Tanaka, *Neurosci. Res.* **16**, 149 (1993); W. A. Fairman, R. J. Vandenberg, J. L. Arriza, M. P. Kavanaugh, S. G. Amara, *Nature* **375**, 599 (1995).
5. J. D. Rothstein *et al.*, *Neuron* **13**, 713 (1994); K. Yamada *et al.*, *NeuroReport* **7**, 2013 (1996).
6. K. Tanaka *et al.*, data not shown.
7. The mouse gene encoding GLT-1 was isolated from a mouse genomic library prepared from 129/SvJ mouse DNA (Stratagene) by hybridization with the 763–base pair (bp) Nco I fragment of the mouse GLT-1 cDNA [Y. Mukainaka, K. Tanaka, T. Hagiwara, K. Wada, *Biochim. Biophys. Acta* **1244**, 233 (1995)] used as a probe. The gene comprised 11 exons spanning more than 78 kb [K. Tanaka *et al.*, *Soc. Neurosci. Abstr.* **21**, 1862 (1995)]. The targeting vector consisted of the 11.6-kb genomic sequence in which the 0.8-kb Not I–Eco RV fragment encoding a part of the transmembrane region of GLT-1 was replaced with the 1.2-kb neomycin gene derived from pMC1 neopolyA. A 1.9-kb herpes simplex virus thymidine kinase gene fragment was attached to the 5′ end of the GLT-1-neomycin fragment for negative selection. E14 ES cells were transfected with Kpn I–digested targeting vector by electroporation and selected with G418 and GANC. ES cell lines with targeted disruption of the GLT-1 gene were identified by Southern blot analysis, and targeted clones were obtained with a frequency of 1/36. Injection of ES cells into blastocysts was performed as described [A. P. McMahon and A. Bradley, *Cell* **62**, 1073 (1990)]. RNA blot analysis was carried out by hybridization of total cerebral RNA (10 μg) with the 785-bp Eco RV–Hind III fragment of the mouse GLT-1 cDNA. Crude membrane preparations from mice cerebra were separated by 5 to 15% gradient SDS–polyacrylamide gel electrophoresis, transferred to nitrocellulose, and analyzed by the ECL detection system (Amersham). The antibody to GLT-1 was raised against the COOH-terminal part of GLT-1 (from Leu^{500} to Lys^{525}).
8. In situ hybridization analysis was performed on the parasagittal brain sections as described [T. Shibata, M. Watanabe, K. Tanaka, K. Wada, Y. Inoue, *NeuroReport* **7**, 705 (1996)]. Antisense oligonucleotide probes were as follows: for GLAST, CACATTATCACCGCGACCAATCGCATGATGGCTTCGTTAAGAGAA; for GLT-1, TCGTCGTTCTTCTTCCCGGGCCCTAGCTGCTTCTTGAGTTTGGGA; for EAAC1, ATCGCCCACAGGCTTCACCTCTTCCCGCTTGGTTTTGTACTGCTGA; and for EAAT4, GCCCCCAGCTCTGAACCATTGTCTGTCCTTACAATTGTCCTTGTCA.
9. Crude synaptosomes were prepared from the cortex, and glutamate transport was measured as described [M. B. Robinson, M. Hunter-Ensor, J. Sinor, *Brain Res.* **544**, 196 (1991)]. The synaptosomal preparation (15 to 30 μg of protein per tube) was incubated with 5×10^5 decay per minute of L-[^{3}H]glutamate (54.1 Ci/mmol; New England Nuclear) and with increasing concentrations of glutamate (0 to 300 μM) for 3 min at 37°C in a final volume of 250 μl. Sodium-dependent uptake was calculated to be the difference between the amount of radioactivity obtained in the presence of Na^+ and the amount obtained in the choline-containing buffer. Experiments were done in triplicate for each concentration. The data were analyzed with a nonlinear least-squares curve-fitting technique.
10. M. A. Rogawski *et al.*, *J. Pharmacol. Exp. Ther.* **249**, 708 (1989).
11. To record EEGs, stainless steel flat electrodes were placed on the parietal and frontal portions of the dura mater. In GLT-1 mutant mice, the EEG recordings were normal in the absence of PTZ.
12. M. A. Kirschner, N. G. Copeland, D. J. Gilbert, N. A. Jenkins, S. G. Amara, *Genomics* **24**, 218 (1994).
13. M. L. Rise, W. N. Frankel, J. M. Coffin, T. N. Seyfried, *Science* **253**, 669 (1991).
14. Wild-type or mutant mice 5 to 7 weeks old were decapitated under halothane anesthesia, and hippocampi were quickly removed. Recordings were made from hippocampal slices (400 μm thick) at 26° to 28°C [T. Manabe, D. J. A. Wyllie, D. J. Perkel, R. A. Nicoll, *J. Neurophysiol.* **70**, 1451 (1993)]. To evoke synaptic responses, stimuli (0.1 Hz) were delivered through fine bipolar tungsten electrodes placed in the stratum radiatum. The non-NMDA component could be isolated by holding the cell at potentials more negative than −80 mV. NMDA receptor–mediated EPSCs were recorded with 6-cyano-7-nitroquinoxaline-2,3-dione (CNQX) (20 μM) present to block non-NMDA receptor–mediated EPSCs, and the membrane potential was clamped at +40 mV to remove the voltage-dependent Mg^{2+} block of the NMDA receptor. The values of the membrane potential were corrected for the liquid-junction potential at the electrode tip (−10 mV). Series and input resistances were monitored throughout the experiment. The time constant of the decaying phase of synaptic currents was calculated by fitting a single exponential curve. CNQX and L-AP5 were obtained from Tocris Cookson (Bristol, U.K.).
15. J. S. Isaacson and R. A. Nicoll, *J. Neurophysiol.* **70**, 2187 (1993).
16. J. D. Clements, R. A. Lester, G. Tong, C. E. Jahr, G. L. Westbrook, *Science* **258**, 1498 (1992).
17. J. I. Wadiche, J. L. Arriza, S. G. Amara, M. P. Kavanaugh, *Neuron* **14**, 1019 (1995).
18. The wild-type and GLT-1 mutant mice were fixed transcardially with 4% paraformaldehyde in 0.1 M sodium phosphate buffer and embedded in paraffin wax. Five-micrometer paraffin sections were stained with toluidine blue for Nissl staining.
19. K. Tanaka *et al.*, data not shown.
20. A. I. Faden, P. Demediuk, S. S. Painter, R. Vink, *Science* **244**, 798 (1989); T. K. McIntosh, R. Vink, H. Soares, R. Hayes, R. Simon, *J. Neurochem.* **55**, 1170 (1990).
21. T. D. Oury, C. A. Piantadois, J. D. Crapo, *J. Biol. Chem.* **268**, 15394 (1993).
22. Mice were anesthetized by intraperitoneal injection of pentobarbital (60 mg/kg). An incision was then made in the scalp, and a metal probe 3 mm in diameter, cooled in liquid nitrogen, was placed on the skull over the left cerebral hemisphere for 10 s. The skin incision was then sutured. After the injury (110 min) the mouse was perfused transcardially with 20 ml of saline. The right (R) and left (L) cerebral hemispheres were separated and immediately weighed (wet weight, *W*). Each hemisphere was then dried at 70°C for 2 days until a constant weight was achieved (dry weight, *D*). An index of edema (*I*) was then calculated as shown in Eq. 1.

$$I = (W/D_L - W/D_R)/(W/D_R) \times 100 \quad (1)$$

This calculation allowed the right hemisphere to serve as a control for the injured left hemisphere in the same mouse.

23. We thank S. Ogawa and Y. Imagawa for the analysis of edema development after cold injury and R. Kado, T. Takahashi, and T. Okada for critical comments on the manuscript. Supported in part by research grants from the Ministry of Education, Science and Culture of Japan; the Ministry of Health and Welfare of Japan; the Science and Technology Agency of Japan; and the Japan Foundation for Neuroscience and Mental Health.

3 January 1997; accepted 2 April 1997

Osmotic Activation of the HOG MAPK Pathway via Ste11p MAPKKK: Scaffold Role of Pbs2p MAPKK

Francesc Posas and Haruo Saito*

Exposure of the yeast *Saccharomyces cerevisiae* to high extracellular osmolarity induces the Sln1p-Ypd1p-Ssk1p two-component osmosensor to activate a mitogen-activated protein (MAP) kinase cascade composed of the Ssk2p and Ssk22p MAP kinase kinase kinases (MAPKKKs), the Pbs2p MAPKK, and the Hog1p MAPK. A second osmosensor, Sho1p, also activated Pbs2p and Hog1p, but did so through the Ste11p MAPKKK. Although Ste11p also participates in the mating pheromone–responsive MAPK cascade, there was no detectable cross talk between these two pathways. The MAPKK Pbs2p bound to the Sho1p osmosensor, the MAPKKK Ste11p, and the MAPK Hog1p. Thus, Pbs2p may serve as a scaffold protein.

MAP kinase cascades are common eukaryotic signaling modules that consist of a MAP kinase (MAPK), a MAPK kinase (MAPKK), and a MAPKK kinase (MAPKKK) (*1*). In *S. cerevisiae*, two independent osmosensors regulate the common HOG (high osmolarity glycerol response) signal transduction pathway, which includes the Pbs2p MAPKK and Hog1p MAPK (*2*–*5*). The Sln1p-Ypd1p-Ssk1p two-component osmosensor uses a multistep phosphorelay mechanism to regulate the redundant MAPKKKs Ssk2p and Ssk22p (*2*, *3*, *6*, *7*). Activated Ssk2p or Ssk22p then phosphorylates and activates the Pbs2p MAPKK. The second osmosensor, Sho1p, contains four transmembrane segments and a COOH-terminal cytoplasmic region with an SRC homology 3 (SH3) domain (*3*). The interaction between an NH_2-terminal proline-rich motif in Pbs2p and the Sho1p SH3

Division of Tumor Immunology, Dana-Farber Cancer Institute, and Department of Biological Chemistry and Molecular Pharmacology, Harvard Medical School, Boston, MA 02115, USA.

*To whom correspondence should be addressed. E-mail: haruo_saito@dfci.harvard.edu

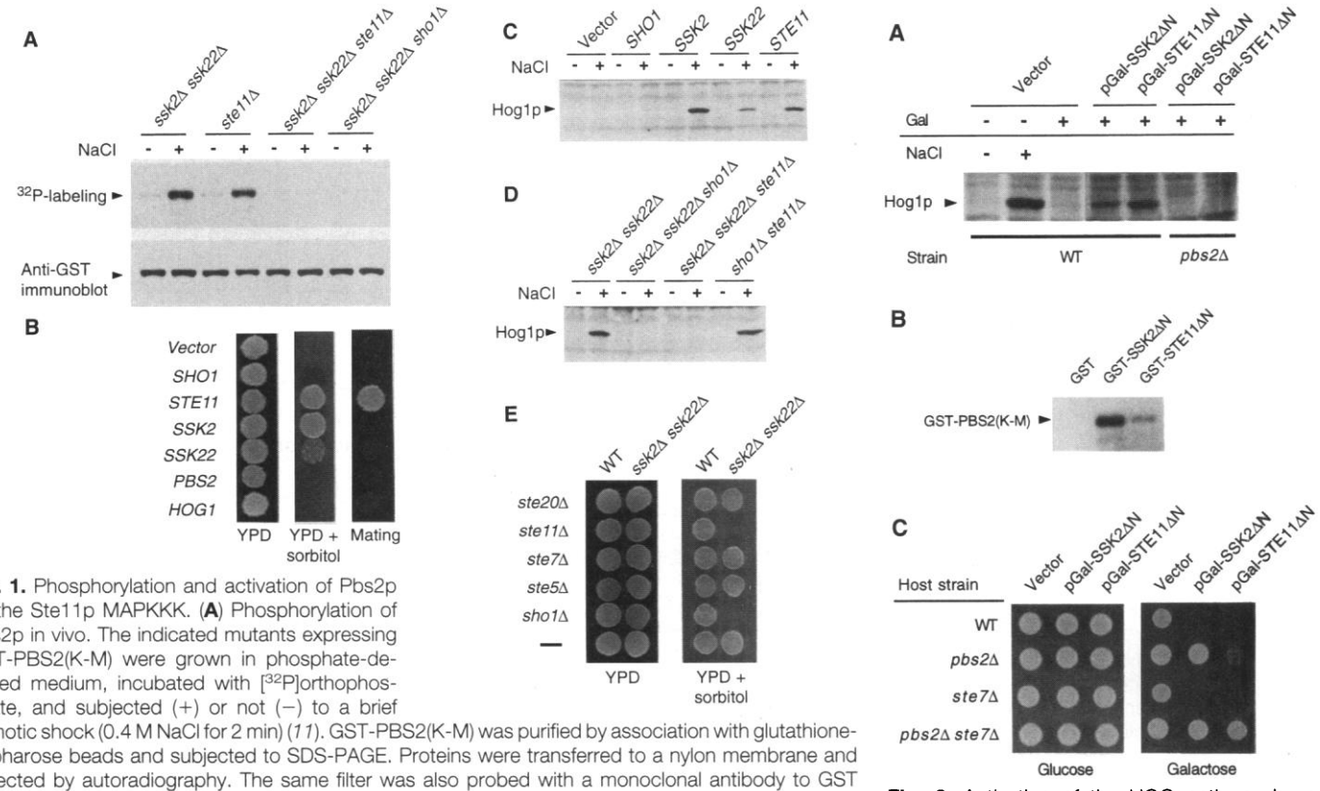

Fig. 1. Phosphorylation and activation of Pbs2p by the Ste11p MAPKKK. (**A**) Phosphorylation of Pbs2p in vivo. The indicated mutants expressing GST-PBS2(K-M) were grown in phosphate-depleted medium, incubated with [^{32}P]orthophosphate, and subjected (+) or not (−) to a brief osmotic shock (0.4 M NaCl for 2 min) (*11*). GST-PBS2(K-M) was purified by association with glutathione-Sepharose beads and subjected to SDS-PAGE. Proteins were transferred to a nylon membrane and detected by autoradiography. The same filter was also probed with a monoclonal antibody to GST (anti-GST). Arrowheads indicate the position of GST-PBS2(K-M). (**B**) Osmosensitivity and sterility of OS-306 (*ssk2Δ ssk22Δ ste11-306*). OS-306 was transformed with centromeric plasmids containing the indicated genes. The transformants were spotted on YPD plates with or without 1.5 M sorbitol. Mating competency was assayed by the replica method (*18*). (**C**) High osmolarity–induced tyrosine phosphorylation of Hog1p in strain FP50 (*MAT**a** ura3 leu2 his3 ssk2::LEU2 ssk22::LEU2 ste11::HIS3*) transformed with plasmids containing the indicated genes. Cells were collected before (−) or 5 min after (+) the addition of NaCl to a final concentration of 0.4 M. Tyrosine-phosphorylated Hog1p was detected by immunoblot analysis with monoclonal antibody 4G10 to phosphotyrosine. (**D**) High osmolarity–induced tyrosine phosphorylation of Hog1p in various mutant strains. Cells were treated as in (C) and tyrosine-phosphorylated Hog1p was detected by immunoblot analysis. (**E**) Osmosensitivity of various mutants. The indicated genes were disrupted (*13*) in the wild-type (WT) strain TM141 (*MAT**a** ura3 leu2 trp1 his3*) and the *ssk2Δ ssk22Δ* strain TM254 (*MAT**a** ura3 leu2 his3 ssk2::LEU2 ssk22::LEU2*), and the osmosensitivity of the resulting cells was tested as in (B).

Fig. 2. Activation of the HOG pathway by a constitutively active Ste11p (STE11ΔN) through Pbs2p phosphorylation. (**A**) Pbs2p-dependent tyrosine phosphorylation of Hog1p induced by the expression of SSK2ΔN or STE11ΔN (*19*). The plasmids pGal-SSK2ΔN, pGal-STE11ΔN, or pYES2 (vector) were introduced into wild-type (WT) strain TM141 or its *pbs2Δ* (*pbs2::LEU2*) derivative. Cells were grown in synthetic medium with raffinose, and the *GAL1* promoter was induced with galactose (*2*). Samples were taken before (−) or 1 hour after (+) addition of galactose. Wild-type cells were treated (+) or not (−) with 0.4 M NaCl for 5 min. Tyrosine-phosphorylated Hog1p was detected by immunoblot analysis with antibody 4G10. (**B**) In vitro phosphorylation of Pbs2p by GST-SSK2ΔN or GST-STE11ΔN. Purified GST fusion proteins were incubated with GST-PBS2(K-M) in the presence of [γ-^{32}P]ATP (adenosine triphosphate) and buffer (*20*). ^{32}P-Labeled GST-PBS2(K-M) was detected by autoradiography after SDS-PAGE. (**C**) Activation of both the mating and HOG pathways by overexpression of STE11ΔN. Host cells were transformed with the plasmids pGal-SSK2ΔN or pGal-STE11ΔN. The transformants were spotted on selective medium containing either glucose or galactose. Growth was scored after 4 days at 30°C.

domain is essential for the activation of Pbs2p by Sho1p (*3*). We now show that the activation of Pbs2p by Sho1p is mediated by the Ste11p MAPKKK, which is also an integral component of the mating pheromone response pathway (*8*–*10*). We propose a mechanism to explain how potential cross talk between the mating and the HOG signaling pathways is prevented.

Phosphorylation of Pbs2p appears to be required for its activation by the Sho1p osmosensor because Pbs2p containing mutations at the activating phosphorylation sites (Ser^{514} → Ala and Thr^{518} → Ala) is not activated by Sho1p (*3*). To test the possibility that a kinase other than Ssk2p and Ssk22p can phosphorylate and activate Pbs2p, we examined Pbs2p phosphorylation in vivo with the glutathione S-transferase (GST) fusion protein GST-PBS2(K-M) (*11*). PBS2(K-M) contains a Lys^{389} → Met mutation that inactivates its kinase activity, and thus it cannot undergo autophosphorylation. In *ssk2Δ ssk22Δ* double-mutant cells, GST-PBS2(K-M) was highly phosphorylated after a brief osmotic shock (Fig. 1A). This phosphorylation event was apparently dependent on the Sho1p osmosensor, because GST-PBS2(K-M) recovered from the *ssk2Δ ssk22Δ sho1Δ* triple mutant after osmotic shock was not phosphorylated (Fig. 1A). These results suggest that a protein kinase other than Ssk2p and Ssk22p can phosphorylate Pbs2p in cells exposed to osmotic shock.

To identify the protein kinase responsible for the Sho1p-mediated phosphorylation of Pbs2p, we screened for mutants on the basis of the assumption that mutational inactivation of the responsible kinase, in conjunction with *ssk2Δ* and *ssk22Δ* mutations, would render the mutant cell incapable of activating Pbs2p and thus would confer osmosensitivity. One such synthetic mutant, OS-306, was sterile as well as osmosensitive. We isolated 20 genomic clones that complemented the osmosensitivity of OS-306, of which 10 contained *SSK2* and another 10 all contained the *STE11* gene (*12*). The *STE11* genomic clones complemented both the

sterility and the osmosensitivity of OS-306 (Fig. 1B). To exclude the possibility that *STE11* was merely acting as a multicopy suppressor of OS-306, we disrupted the *STE11* gene in an *ssk2Δ ssk22Δ* strain. Several independently isolated *ssk2Δ ssk22Δ ste11Δ* triple mutants were all sterile and osmosensitive (Fig. 1E). Disruption of *STE11* alone had no effect on Pbs2p phosphorylation in vivo, but Pbs2p was not phosphorylated in response to osmotic shock in an *ssk2Δ ssk22Δ ste11Δ* triple mutant (Fig. 1A). Thus, Ste11p contributes to the activation of Pbs2p.

Tyrosine phosphorylation of Hog1p is a sensitive measure of the activation state of Pbs2p (*2*, *5*). However, Hog1p phosphorylation was not observed in response to osmotic shock in *ssk2Δ ssk22Δ ste11Δ* cells, indicating that this triple mutant has completely lost the capacity to activate Pbs2p (Fig. 1C). Transformation of the *ssk2Δ ssk22Δ ste11Δ* triple mutant with a plasmid containing either $SSK2^+$, $SSK22^+$, or $STE11^+$, but not $SHO1^+$, restored tyrosine phosphorylation of Hog1p in response to osmotic shock, indicating the redundant roles of Ssk2p, Ssk22p, and Ste11p in Pbs2p activation. Consistent with the notion that *sho1Δ* and *ste11Δ* mutations inactivate the same upstream signaling branch in the HOG pathway, neither *ssk2Δ ssk22Δ sho1Δ* nor *ssk2Δ ssk22Δ ste11Δ* triple-mutant cells showed tyrosine phosphorylation of Hog1p in response to osmotic shock (Fig. 1D). In a *sho1Δ ste11Δ* double mutant, in which *SSK2* and *SSK22* are functional, tyrosine phosphorylation of Hog1p in response to osmotic shock was detected (Fig. 1D).

Because Ste11p is a MAPKKK for the mating pheromone response pathway (*9*, *10*), we tested whether other components in the mating pathway also participate in the HOG pathway. Thus, we disrupted either *STE20*, *STE11*, *STE7*, *STE5*, or the control *SHO1* gene in an *ssk2Δ ssk22Δ* background (*13*). Only the *ste11Δ* and *sho1Δ* mutations were synthetically osmosensitive with *ssk2Δ ssk22Δ* (Fig. 1E). Furthermore, disruption of two other genes that encode protein kinases similar to Ste20p—CLA4 and *YOL113*—had no effect on osmosensitivity (*14*). Thus, *STE11* may be the only gene shared between the mating and the HOG pathways.

Kinases in the MAPKKK family can be constitutively activated by eliminating their NH_2-terminal noncatalytic domains (*9*). Indeed, expression of Ssk2p or Ste11p with NH_2-terminal truncations (SSK2ΔN and STE11ΔN, respectively) resulted in Pbs2p-mediated tyrosine phosphorylation of Hog1p in the absence of osmotic stress (Fig. 2A). Thus, both SSK2ΔN and STE11ΔN can activate Pbs2p in the absence of upstream stimuli. Both GST-STE11ΔN and GST-SSK2ΔN proteins also efficiently phosphorylated the GST-PBS2(K-M) protein in vitro (Fig. 2B).

Continuous activation of the Hog1p MAPK by SSK2ΔN is lethal to yeast cells, and this lethality is suppressed by disrup-

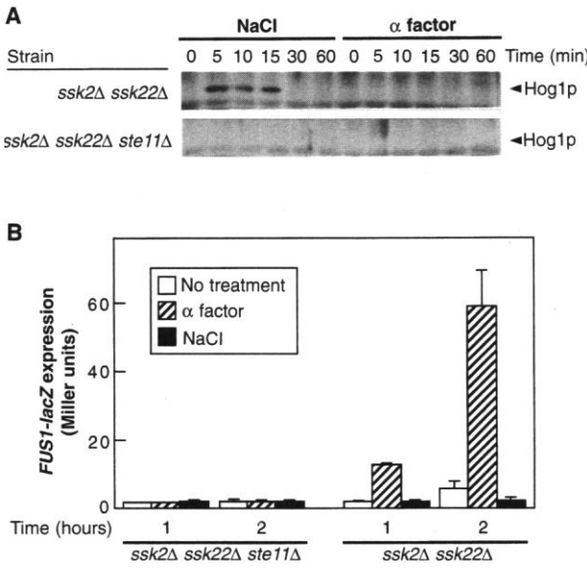

Fig. 3. Lack of cross talk between the mating and HOG pathways. (**A**) Time course of Hog1p tyrosine phosphorylation. Yeast strains TM254 (*MATa ssk2Δ ssk22Δ*) or FP50 (*MATa ssk2Δ ssk22Δ ste11Δ*) were exposed to 0.4 M NaCl or 5 μM α factor for the indicated times, and tyrosine-phosphorylated Hog1p was detected by immunoblot analysis with antibody 4G10. (**B**) Expression of *FUS1-lacZ*. TM254 or FP50 strains were transformed with the pSB231 (*FUS1-lacZ*) reporter plasmid (*15*). Transformants were grown to exponential phase in YPD buffered at pH 3.5 (*21*) and exposed to 0.4 M NaCl or 5 μM α factor for the indicated times. β-Galactosidase activity was measured and expressed in Miller units (*22*). Data are means + SD of 12 assays (triplicate determinations with four independent transformants).

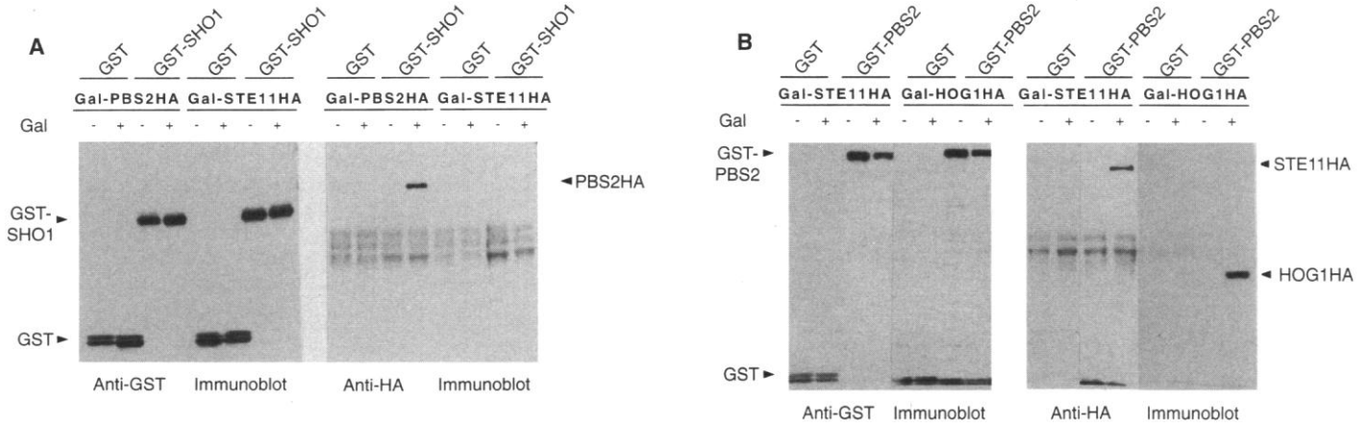

Fig. 4. Association of Pbs2p with Sho1p, Ste11p, and Hog1p. (**A**) Coprecipitation of hemagglutinin (HA)–tagged Pbs2p (PBS2HA) with GST-SHO1. The wild-type yeast strain TM141 was cotransformed with either the p426TEG (GST) or p426TEG-SHO1 (GST-SHO1) plasmids, and DNA encoding either HA-tagged Pbs2p (Gal-PBS2HA) or Ste11p (Gal-STE11HA) under the control of the *GAL1* promoter in the YCplF vector (*23*). Cells were grown in glucose (−) or galactose (+), the latter to induce expression of PBS2HA or STE11HA. Cells were lysed, and proteins were purified by association with glutathione-Sepharose beads (*24*) and subjected to immunoblot analysis with antibodies to GST (anti-GST) or to HA (anti-HA). (**B**) Coprecipitation of STE11HA and HOG1HA with GST-PBS2. TM141 was cotransformed with either p426TEG vector (GST) or p426TEG-PBS2 (GST-PBS2) (this plasmid contains the catalytically inactive $Lys^{389} \rightarrow$ Met mutation to prevent the toxicity of Pbs2p overexpression), and DNA encoding either HA-tagged Ste11p (Gal-STE11HA) or Hog1p (Gal-HOG1HA) under the control of the *GAL1* promoter in the YCplF vector. Cells and samples were processed as in (A).

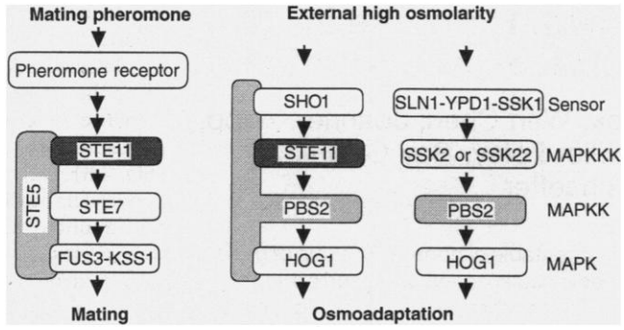

Fig. 5. Schematic model of the pheromone response pathway and the HOG signal transduction pathway. Pbs2p appears to serve as a scaffold protein that holds Sho1p, Ste11p, and Hog1p in a signaling complex, whereas Ste5p holds Ste11p, Ste7p, and Fus3p-Kss1p in a separate complex.

tion of the *PBS2* gene (*3*). Expression of STE11ΔN was also toxic to cells (Fig. 2C). The STE11ΔN lethality was suppressed partially by the *pbs2Δ* mutation and completely by the *ste7Δ pbs2Δ* double mutation. In contrast, *ste7Δ* alone had little suppressive effect. Thus, the STE11ΔN lethality is caused by the hyperactivation of both the mating pheromone pathway and the HOG pathway.

We investigated whether the activation of Ste11p by osmotic stress results in the activation of mating responses and whether activation of Ste11p by mating factors results in activation of the HOG pathway. To assess activation of the mating pathway, we measured the expression of the *FUS1* gene with a *FUS1-lacZ* promoter fusion construct (*15*). Activation of the HOG pathway was assessed by measuring tyrosine phosphorylation of Hog1p. These experiments were performed with *ssk2Δ ssk22Δ* double-mutant cells, so that the activation of the Pbs2p MAPKK was dependent solely on the Ste11p MAPKKK. The α mating factor induced expression of *FUS1-lacZ*, but not tyrosine phosphorylation of Hog1p (Fig. 3). In contrast, osmotic shock induced tyrosine phosphorylation of Hog1p but not *FUS1-lacZ* expression. In *ssk2Δ ssk22Δ ste11Δ* triple-mutant cells, no response to either the mating factor or osmotic shock was detected. Thus, although the Ste11p MAPKKK participates in both the mating and HOG pathways, there is little or no cross talk between these pathways.

The scaffold protein Ste5p interacts with the Ste11p MAPKKK, Ste7p MAPKK, Fus3p-Kss1p MAPK (*16*), and G protein βγ subunits (*17*). Thus, the complex formed around Ste5p may allow the incoming signal from the mating factor receptor to flow only through this complex. The previous observation that the Sho1p osmosensor interacts with Pbs2p suggests that another signaling complex may be formed by the components of the HOG signaling pathway (*3*). Indeed, coprecipitation experiments revealed that Sho1p was associated with Pbs2p but not with Ste11p in intact cells (Fig. 4A), and that Pbs2p interacts with both Ste11p and Hog1p (Fig. 4B).

Our results are consistent with the formation of a multiprotein complex that includes Sho1p, Ste11p, Pbs2p, and Hog1p, although it remains to be shown that these interactions occur simultaneously. Formation of such a multiprotein complex would restrict the osmotic stress–activated Ste11p MAPKKK to phosphorylating only the Pbs2p MAPKK, like the Ste5p complex ensures that the mating pheromone–activated Ste11p MAPKKK phosphorylates only the Ste7p MAPKK (Fig. 5). In this sense, both Ste5p and Pbs2p appear to serve a similar scaffold function, even though they are not structurally related. Given that several distinct MAP kinase cascades coexist in mammalian cells, formation of similar multiprotein complexes may be a general mechanism to prevent inappropriate cross talk.

REFERENCES AND NOTES

1. A. J. Waskiewicz and J. A. Cooper, *Curr. Opin. Cell Biol.* **7**, 798 (1995); I. Herskowitz, *Cell* **80**, 187 (1995).
2. T. Maeda, S. M. Wurgler-Murphy, H. Saito, *Nature* **369**, 242 (1994).
3. T. Maeda, M. Takekawa, H. Saito, *Science* **269**, 554 (1995).
4. G. Boguslawski and J. O. Polazzi, *Proc. Natl. Acad. Sci. U.S.A.* **84**, 5848 (1987); J. Albertyn, S. Hohmann, J. M. Thevelein, B. A. Prior, *Mol. Cell. Biol.* **14**, 4135 (1994).
5. J. L. Brewster, T. de Valoir, N. D. Dwyer, E. Winter, M. C. Gustin, *Science* **259**, 1760 (1993).
6. I. M. Ota and A. Varshavsky, *ibid.* **262**, 566 (1993).
7. F. Posas *et al.*, *Cell* **86**, 865 (1996).
8. N. Rhodes, L. Connell, B. Errede, *Genes Dev.* **4**, 1862 (1990).
9. B. R. Cairns, S. W. Ramer, R. D. Kornberg, *ibid.* **6**, 1305 (1992).
10. A. Gartner, K. Nasmyth, G. Ammerer, *ibid.*, p. 1280; B. J. Stevenson, N. Rhodes, B. Errede, G. F. Sprague, *ibid.*, p. 1293.
11. In vivo protein labeling was performed essentially as described (*7*). Cells were grown in phosphate-depleted medium [J. R. Warner, *Methods Enzymol.* **194**, 423 (1991)], incubated with [^{32}P]orthophosphate (0.75 mCi/ml, 9000 Ci/mmol) for 15 min at 30°C, and treated with 0.4 M NaCl for 2 min before harvesting. GST-PBS2(K-M) was purified with glutathione-Sepharose (Pharmacia) [D. B. Smith and K. S. Johnson, *Gene* **67**, 31 (1988)] followed by SDS–polyacrylamide gel electrophoresis (PAGE).
12. OS-306 (*MATa ura3 leu2 his3 ssk2::LEU2 ssk22::LEU2 ste11-306*) was transformed with a yeast genomic DNA library in YCp50 (*URA3*$^+$ marker). Ura$^+$ transformants were replica-plated onto YPD (yeast extract, peptone, and dextrose) plates containing 1.5 M sorbitol, and 20 osmoresistant colonies were selected. Plasmids recovered from the osmoresistant transformants revealed that 10 contained *SSK2* and another 10 contained the complete *STE11* open reading frame.
13. Genes were disrupted with the *HIS3*$^+$ marker by the microhomology-mediated polymerase chain reaction (PCR) targeting method [P. Manivasakam, S. C. Weber, J. McElver, R. Schiestl, *Nucleic Acids Res.* **23**, 2799 (1995)]. The structure of disrupted genes was verified by PCR analysis of chromosomal DNA with specific primers. For the *STE* gene disruptants, their sterile phenotype was also confirmed by the replica-plate mating method (*18*).
14. F. Posas and H. Saito, unpublished observations.
15. G. McCaffrey, F. J. Clay, K. Kelsay, G. F. Sprague, *Mol. Cell. Biol.* **7**, 2680 (1987).
16. J. E. Kranz, B. Satterberg, E. A. Elion, *Genes Dev.* **8**, 313 (1994); S. Marcus, A. Polverino, M. Barr, M. Wigler, *Proc. Natl. Acad. Sci. U.S.A.* **91**, 7762 (1994); J. A. Printen and G. F. Sprague, *Genetics* **138**, 609 (1994); K. Y. Choi, B. Satterberg, D. M. Lyons, E. A. Elion, *Cell* **78**, 499 (1994).
17. M. S. Whiteway *et al.*, *Science* **269**, 1572 (1995).
18. G. F. Sprague, *Methods Enzymol.* **194**, 77 (1991).
19. The fragment of *STE11* DNA that encodes from Lys^{364} to the COOH-terminus was cloned into the *GAL1* promoter expression plasmid pYES2 (*URA3*$^+$ marker) to construct pGal-STE11ΔN. pGal-SSK2ΔN was as described previously and encodes Met^{1173} to the COOH-terminus of Ssk2p (*3*).
20. GST, GST-SSK2ΔN, and GST-PBS2(K-M) were each expressed in *Escherichia coli* DH5. GST-STE11ΔN was expressed in yeast, because the same construct expressed in *E. coli* was catalytically inactive [A. M. Neiman and I. Herskowitz, *Proc. Natl. Acad. Sci. U.S.A.* **91**, 3398 (1994)]. GST fusion proteins were purified as described (*7*). For the in vitro kinase reactions, 0.6 μg of purified GST, GST-SSK2ΔN, or GST-STE11ΔN was incubated for 20 min at 30°C with 1.5 μg of GST-PBS2(K-M) in a kinase buffer [50 mM tris-HCl (pH 7.5), 10 mM $MgCl_2$, 2 mM dithiothreitol, and 100 μM [γ-^{32}P]ATP (50 Ci/mmol)]. Reactions were stopped by the addition of 2× SDS sample buffer (*7*), and samples were subjected to SDS-PAGE and autoradiography.
21. E. M. Ciejek and J. Thorner, *Cell* **18**, 623 (1979).
22. R. R. Yocum, S. Hanley, R. J. West, M. Ptashne, *Mol. Cell. Biol.* **4**, 1985 (1984).
23. The p426TEG vector contains the GST coding sequence under the control of the constitutive *TEF1* promoter (M. Takekawa and H. Saito, unpublished data). YCpIF plasmids used for the construction of HA-tagged fusion proteins have been described [P. K. Foreman and R. W. Davis, *Gene* **144**, 63 (1994)]. The GST-SHO1 hybrid construct contains only the cytoplasmic region of Sho1p (Asn^{170} to the COOH-terminus). Other constructs (GST-PBS2, PBS2HA, STE11HA, and HOG1HA) contain the full-length coding sequences of the respective genes.
24. Cell extracts were prepared essentially as described (*7*). Protein concentration was determined with the Bio-Rad protein assay. Cell extracts (750 μg) were incubated for 5 hours at 4°C with 50 μl of glutathione-Sepharose beads in a buffer containing 150 mM NaCl. The beads were washed extensively with the same buffer, and bound proteins were separated by SDS-PAGE, transferred to nitrocellulose, incubated with the indicated antibodies, and visualized by chemiluminescence.

25. We thank E. A. Witten for technical assistance, M. Takekawa and S. I. Reed for plasmids, and M. Streuli for comments on the manuscript. Supported by grants GM50909 and GM53415 from NIH (H.S.) and a postdoctoral fellowship from la Dirección General de Investigación Científica y Técnica of the Spanish government (F.P.).

13 February 1997; accepted 17 April 1997